

## Observation of Neutron Bursts Produced by Laboratory High-Voltage Atmospheric Discharge

A. V. Agafonov,<sup>1</sup> A. V. Bagulya,<sup>1</sup> O. D. Dalkarov,<sup>1,2</sup> M. A. Negodaev,<sup>1</sup> A. V. Oginov,<sup>1,\*</sup> A. S. Rusetskiy,<sup>1</sup>  
V. A. Ryabov,<sup>1</sup> and K. V. Shpakov<sup>1</sup>

<sup>1</sup>*P.N. Lebedev Physical Institute of the Russian Academy of Sciences (FIAN), Leninsky Prospekt, 53, Moscow 119991, Russia*

<sup>2</sup>*Centre for Fundamental Research (MIEM NRU HSE), Myasnizkaya, 20, Moscow 101000, Russia*

(Received 10 April 2013; published 12 September 2013)

For the first time the emission of neutron bursts in the process of high-voltage discharge in air was observed. Experiments were carried out at an average electric field strength of  $\sim 1 \text{ MV} \cdot \text{m}^{-1}$  and discharge current of  $\sim 10 \text{ kA}$ . Two independent methods (CR-39 track detectors and plastic scintillation detectors) registered neutrons within the range from thermal energies up to energies above  $10 \text{ MeV}$  and with an average flux density of  $\geq 10^6 \text{ cm}^{-2}$  per shot inside the discharge zone. Neutron generation occurs at the initial phase of the discharge and correlates with x-ray generation. The data obtained allow us to assume that during the discharge fast neutrons are mainly produced.

DOI: 10.1103/PhysRevLett.111.115003

PACS numbers: 52.80.Mg, 24.10.-i, 28.20.-v, 29.40.Gx

*Introduction.*—Intense fluxes of gamma radiation, electrons, and even positrons and neutrons in a thunderstorm atmosphere are observed at different types of atmospheric phenomena: terrestrial gamma flashes (TGF) [1], new forms of discharges between the atmosphere and the ionosphere (sprites, elves, and blue jets) [2], as well as in conventional thunderstorm discharges. At present, evidence of neutron flux enhancement in lightning discharges of the atmosphere has been obtained in a number of experiments at sea level [3–5], high elevations [6–10], and even in near space [11]. These experiments led to observations of a neutron flux excess over the cosmic background during thunderstorm activity. The registered neutron energy was in the range from thermal (0.01 eV) to fast (tens of MeV). In Ref. [12] the observed intense neutron production in TGF's ( $\sim 10^{12}$  neutrons) corresponded to a ground-level neutron fluence of  $(0.03\text{--}1) \times 10^4 \text{ m}^{-2}$ .

The nuclear fusion reactions  ${}^2\text{H}({}^2\text{H}, n){}^3\text{He}$  in the lightning channel [4], the reaction  ${}^{12}\text{C}({}^2\text{H}, n){}^{13}\text{N}$ ,  ${}^{14}\text{N}({}^2\text{H}, n){}^{15}\text{O}$  [13], and the photonuclear ( $\gamma, n$ ) reactions [14] have been considered as possible mechanisms leading to the formation of a neutron flux in a thunderstorm atmosphere. However, there is no satisfactory explanation for the aggregate of existing experimental results. Therefore, these experiments on studying the neutron emission in laboratory conditions, in high-voltage discharges in the air, which are similar to conditions observed in a natural storm, were deemed to be important.

It is necessary to ensure control of the main parameters of the medium in which the discharge occurs in order to study in detail the issues of initiation and temporal structure of a lightning discharge to identify the characteristic accompanying radiation of the discharge. Measurements on balloons, rockets, and airplanes demonstrated that the maximum electric field in thunderclouds usually does not exceed  $3\text{--}9 \text{ kV} \cdot \text{cm}^{-1}$  [1,2,15], which is well below the breakdown threshold of dry air at high

altitudes ( $\sim 10 \text{ kV} \cdot \text{cm}^{-1}$ ) and ground level ( $\sim 25 \text{ kV} \cdot \text{cm}^{-1}$ ). In a thunderstorm cloud, however, the discharge develops in moist air. Perhaps the threshold field is achieved in a compact spatial domain due to the increase of the field on water droplets, over a too short period of time, so that the usual field sensors do not provide the required spatial and temporal resolution for registration. An alternative explanation for the initiation of a discharge in a weak field ( $2.5\text{--}3 \text{ kV} \cdot \text{cm}^{-1}$ ) is the development of an avalanche of fast (so-called runaway) electrons [16]. Typical currents of lightning discharges are tens of kiloamperes [17].

Our experimental laboratory setup covers the domain of above mentioned parameters and permits us to reproduce and change most terms of atmospheric discharge to vary the strength of the average and local electric field, current, and humidity, and to create within the discharge gap finely dispersed particles of water from the environment, as well as using an external electron source to investigate the role of the seed of energetic charged particles.

*Experimental setup.*—The experiments were carried out with a high current electron beam accelerator ERG, reconstructed for studying the high-voltage discharge in air [18]. The scheme of the experiment is shown in Fig. 1(a). The voltage amplitude, up to  $1 \text{ MV}$  from the screened Marx generator with a stored energy of  $60 \text{ kJ}$ , is fed through the entranced oil-air isolator to a duralumin flange with replaceable electrodes (cathode), and provides a discharge current of  $10\text{--}15 \text{ kA}$  in air. The diameter of the external grounded cylindrical conductor limits the allowable distance between the cathode and the anode at a level of  $1 \text{ m}$ . The anode flange can be moved along the axis of the system for a smooth change in the gap. The anodes and cathodes used the same set of replaceable electrodes.

Electrophysical diagnostics included the recording of the current waveforms (anode shunt, Rogowski coils) and voltage (active and capacitive divider), and azimuthal magnetic field probes with a bandwidth of  $200 \text{ MHz}$ . The

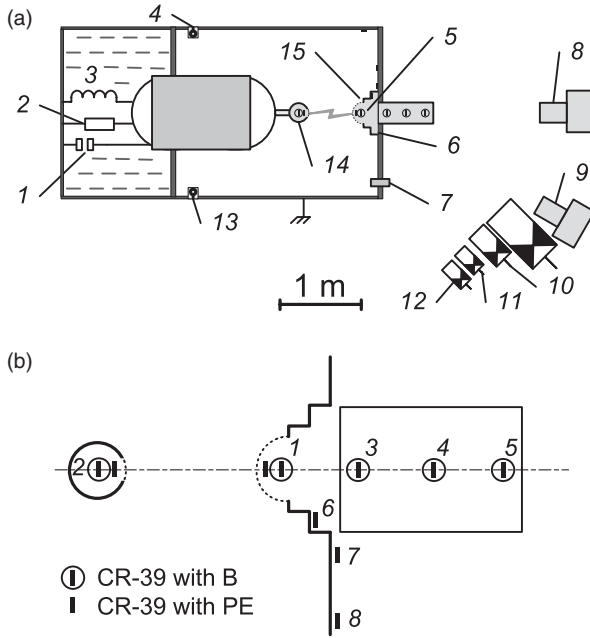


FIG. 1. The scheme of the laboratory experiment. (a) Layout of diagnostics: 1, 2, capacitive and active dividers; 3, high voltage input from Marx generator; 4, 13, magnetic probes; 5, track detectors; 6, anode shunt; 7, Rogowski coil; 8, 9, integral cameras; 10, scintillation detectors; 11, UV radiation detector; 12, PMT to visible light; 14, cathode; 15, anode. (b) Layout of CR-39 track detectors: 1, inside the anode; 2, inside the cathode; 3, 4, 5, axially placed in water; 6, 7, 8, radially placed at different distances from the discharge.

channel formation of the discharge is monitored using integral shooting in the optical range from two angles.

To register an integral neutron flux the CR-39 track detectors, produced by the Fukuvi Chemical Industry Company, which are insensitive to the electromagnetic radiation, have been used. The CR-39 track detectors are located near the zone of discharge as shown in Fig. 1(b).

Calibration of the CR-39 detector by charged particles has been carried out on the beam of protons from an electrostatic accelerator ( $E_p = 0.5\text{--}3.0$  MeV), with standard  $\alpha$  sources ( $E_\alpha = 2\text{--}7.7$  MeV), and on the cyclotron beam ( $E_\alpha = 8\text{--}30$  MeV) at Skobel'syn Institute of Nuclear Physics of Moscow State University. Irradiated detectors were etched in a 6M NaOH solution in  $\text{H}_2\text{O}$  at a temperature of 70 C for 7 hours. Procedure of the track detector calibration is considered in Ref. [19].

The neutron calibration of the CR-39 detector was performed using a  $^{252}\text{Cf}$  source with an activity of  $3 \times 10^4 \text{ n} \cdot \text{s}^{-1}$  in a solid angle of  $4\pi$ . A detector with a radiator of  $120 \mu\text{m}$  polyethylene (detectors with PE in Fig. 1) was used. Recoil protons produced by fast neutrons were registered by the track detector. The calibration measurements showed that the diameters of the proton tracks are in the range of  $4\text{--}8 \mu\text{m}$ . The average efficiency of fast

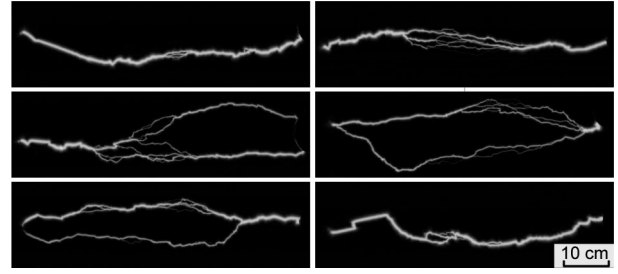
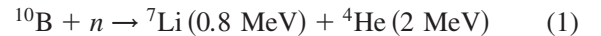


FIG. 2. Different shapes of atmospheric discharge in the experiment.

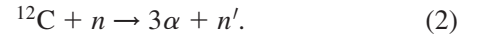
neutron registration by the CR-39 detector was  $\eta_{n1} = 6 \times 10^{-5}$ .

For the registration of thermal neutrons by the reaction



the detectors were placed in a 20% solution of  $\text{Na}_2\text{B}_4\text{O}_7$  in glycerol (detectors with B in Fig. 1). The neutrons were registered by counting the tracks of  $\alpha$  particles with  $E_\alpha < 2$  MeV, which, according to the calibration, have diameters of  $10\text{--}12 \mu\text{m}$ . The average efficiency of thermal neutron registration by the CR-39 detector was  $\eta_{n2} = 1.4 \times 10^{-6}$ .

Fast neutrons of energy  $E_n > 10$  MeV were detected by the reaction of



With the energy threshold of about 10 MeV a characteristic signature of desintegration of the nucleus  $^{12}\text{C}$  presents three  $\alpha$  particles, and their tracks come from a single point. The average efficiency of registration of the fast neutrons by reaction (2) using the CR-39 detector with a  $120 \mu\text{m}$  PE radiator was  $\eta_{n3} = 1.2 \times 10^{-6}$  [20].

The registration of neutron emission in the real-time mode was performed by plastic scintillation detectors. For the detection of fast neutrons and x rays POPOP doped polystyrene scintillators were used. The scintillators have an active area of  $15 \times 15 \text{ cm}^2$  and thickness of 5.5 cm. Signals were registered by a four-channel digital storage oscilloscope with a 1 GHz bandwidth. The intrinsic efficiency of the detector to fast neutrons, measured with a  $^{252}\text{Cf}$  source, was equal to  $\eta_{\text{int}} = 0.17$ .

*Results.*—Integral images of discharges—laboratory lightning—obtained by camera 9 [see Fig. 1(a)] are shown in Fig. 2. As in nature, typical features of lightning are revealed: linear, forked, steplike leader channels, etc.

In a series of 180 shots the CR-39 track detectors, placed inside the spherical anode and cathode, showed an excess of neutron flux over the background. Track diameter distributions for the charged particles in detectors are shown in Fig. 3. Round-shaped tracks with an angle of incidence close to the normal have been chosen. The CR-39 detector with a PE radiator of  $120 \mu\text{m}$ , which was placed inside the anode, revealed the following: an  $\sim 5$  times excess of tracks

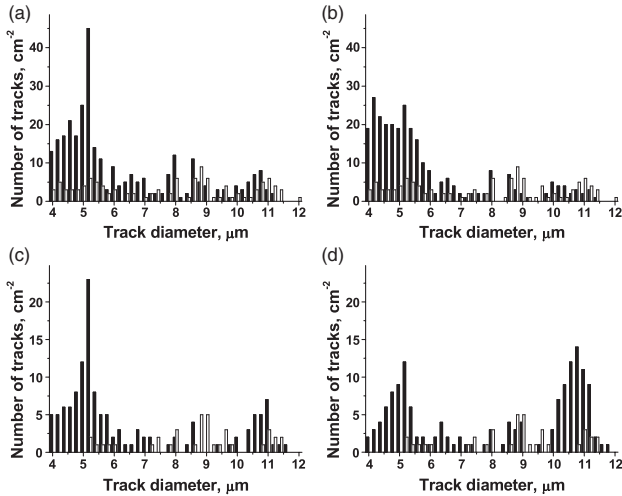


FIG. 3. Total distribution of track diameters. (a),(b) Detectors with radiators of 120  $\mu\text{m}$  polyethylene, located in the anode (position 1) and in the cathode (position 2). (c) Detectors with radiators of 20% solution of  $\text{Na}_2\text{B}_4\text{O}_7$  in glycerol (position 1). (d) Detectors of the 20% solution of  $\text{Na}_2\text{B}_4\text{O}_7$  in glycerol with additional water moderator, placed near the anode (position 3). Dark columns correspond to the results of the experiment, and light columns to the relevant background detectors, placed 10 m in from the discharge. All positions are in accordance with Fig. 1(b).

above the background within the range of recoil proton diameters of 4–6  $\mu\text{m}$  [see Fig. 3(a)]. This excess should correspond to the average fast neutron flux in the location of detector  $\langle n_{n1} \rangle \geq 2 \times 10^5 \text{ cm}^{-2}$  per shot. A similar detector, located inside the cathode, also showed an excess above the background in the same range [Fig. 3(b)]. The average flux of fast neutrons, estimated by the recoil protons, in the detector area was  $\langle n_{n1} \rangle \geq 3 \times 10^5 \text{ cm}^{-2}$  per shot.

The detector inside the anode placed in a 20% solution of  $\text{Na}_2\text{B}_4\text{O}_7$  in glycerol also showed an excess above the background [see Fig. 3(c)] in the 10–12  $\mu\text{m}$  range of diameters of  $\alpha$ -particle tracks ( $E_\alpha < 2 \text{ MeV}$ ). The average thermal neutron flux in the detector area, estimated by reaction (1), was  $\langle n_{n2} \rangle \geq 6 \times 10^5 \text{ cm}^{-2}$  per shot. A significant excess above the background in the 4–6  $\mu\text{m}$  range of the diameters of the recoil proton tracks was also observed. Comparison of the data from detectors 1 and 3 showed that the thermal neutron flux in the far detector [see Fig. 3(d)] is

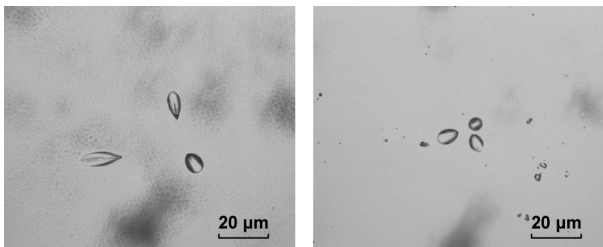


FIG. 4. Typical photomicrographs of the events of  $^{12}\text{C}$  nucleus desintegration into three  $\alpha$  particles (the size of the image is  $130 \times 100 \mu\text{m}^2$ ).

greater. Probably, the fast neutrons are primary in discharge, and then they slow down in the water moderator up to thermal energies.

A very important result is related to the direct observation of the desintegration of the  $^{12}\text{C}$  nucleus into three  $\alpha$  particles. Clear evidence of such events was observed on detectors located near the discharge area. For example, at detector 1 (2  $\text{cm}^2$ ), placed near the anode, there were 10 observed events of the desintegration of the  $^{12}\text{C}$  nucleus into three  $\alpha$  particles (see Fig. 4). Therefore the number of  $3\alpha$  events was  $N_{3\alpha} = 5 \text{ cm}^{-2}$  at the background  $N_{\text{bg}3\alpha} = 0.2 \text{ cm}^{-2}$ ; i.e., the confidence level of the effect of  $^{12}\text{C}$  nucleus desintegration is more than  $10\sigma$ . The average neutron flux of energy  $E_n > 10 \text{ MeV}$  in the detector area, estimated by reaction (2), was  $\langle n_{n3} \rangle \geq 1.4 \times 10^5 \text{ cm}^{-2}$  per shot. On different detectors, located near the discharge,  $N_{3\alpha} = 1\text{--}4 \text{ cm}^{-2}$ .

The CR-39 statistics (detectors with radiators of 120  $\mu\text{m}$  polyethylene at positions 1, 6, 7, 8) indicate an exponential drop [ $\exp(-r/18.4)$ ] of the fast neutron flux with distance  $r$  (cm) from the first detector placed inside the anode. The flux drops more slowly than  $1/r^2$  behavior. The observed deviation may be explained as a case of a neutron source distributed inside the anode-cathode gap.

The observation of neutron signals with plastic scintillation detectors is shown in Fig. 5(a). The detectors are located at a distance of  $\sim 150 \text{ cm}$  from the discharge zone. One of the detectors was shielded by 50  $\mu\text{m}$  Al foil and could detect the pulses from the x rays ( $E_\gamma > 10 \text{ keV}$ ) and neutrons ( $E_n > 1 \text{ MeV}$ ). The other one had an additional 10 cm thick Pb shield. During a discharge both detectors

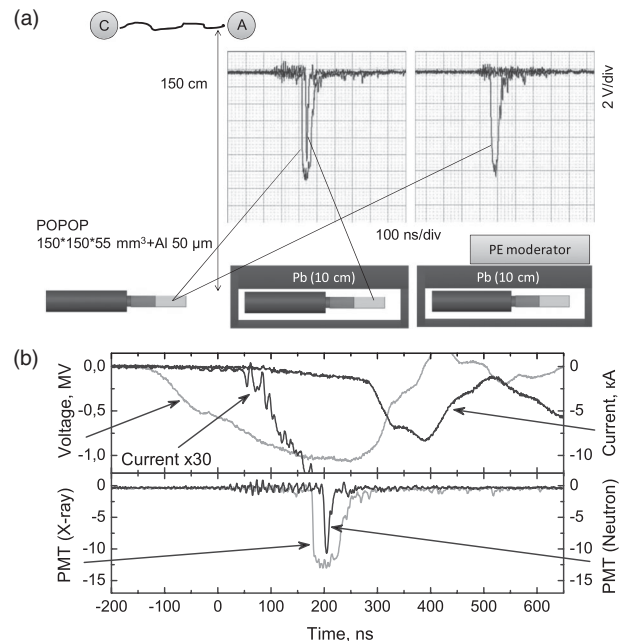


FIG. 5. Scheme of real-time observation: (a) neutron signals, (b) oscillograms of voltage, current, x rays, and neutrons.

TABLE I. Distribution of events over set of observations. All events of amplitude exceeding background by 10% were included.

Gap distance L (cm)	Mean electric field E (kV · cm <sup>-1</sup> )	Number of shots N	Percentage of PMT pulses		
			(No x ray & neutron)	(X ray)	(X ray + neutron)
60	17	90	57%	43%	25%
45	22	90	47%	53%	30%

indicated the time structure of the signals. The start signal (presumably from fast neutrons) in the second detector with the protection of 10 cm of Pb was delayed relative to the first signal (x rays) by 35 ns. Using a time-of-flight estimation gave the neutron energy  $E_n \sim 10$  MeV. The forms of the neutron pulses were about the same for all events. No neutron pulses were observed out of the x-ray pulse. The width and amplitude of the neutron pulses changed in the wide region inside the x-ray pulse. The time delay of the neutron pulse relative to the x-ray pulse changed in the narrower region. It allowed estimation of the energy range of neutrons, but not the locus. Under the assumption that x rays and neutrons are generated simultaneously, the mean energy of the neutrons equals  $15 \pm 7$  MeV.

Taking into account the geometric factor ( $8 \times 10^{-4}$ ) and detection efficiency, the fast fraction of the neutron flux density at the location of the detector is  $\langle n_{n4} \rangle \sim 2$  cm<sup>-2</sup> per shot. It is less than the flux density estimated by reaction (2) by 5 orders due to the different distances from the discharge. The track detectors are placed very close or inside the discharge zone just as the scintillation detectors are located at a distance of 150 cm from the track detectors placed inside the electrodes. No one has previously placed detectors inside the discharge zone in laboratory experiments. If the size of the emission area of the neutrons is much less than the length of the discharge, then that could be the reason why neutrons from the laboratory atmospheric discharge were not observed. The flux drops inversely proportional to the distance squared and its value at the location of the far detectors is rather small. At the time both the track and plastic scintillators detectors “see” the whole gap and the locus (or loci) of neutron emission cannot be defined.

An additional neutron moderator (20 cm of polyethylene) leads to the absence of a signal from fast neutrons at the second detector. This corresponds with the assumption of fast neutron emission. As shown in Fig. 5(b), neutron bursts occur on the prepulse current prior to the formation of the discharge. At the moment of neutron generation the prepulse current amplitude is  $\approx 30$  times smaller than the amplitude of the main current pulse.

In Table I the rates of events with neutrons and x rays are presented. The number of events with neutrons weakly depends on the mean electric field in our experimental conditions and averages 25%–30%. All events with neutron signals are accompanied by x-ray signals.

*Conclusion.*—For the first time in a laboratory experiment during high-voltage atmospheric discharge neutron emission was observed. The energies of neutrons within the range from thermal up to fast are detected; the contribution of fast neutrons in the total flux is a significant part. It should be emphasized that neutron emission occurs at the very beginning of the discharge and is strongly correlated with x-ray radiation. No neutron pulses were observed out of the x-ray pulse. The fast neutron flux drops exponentially and more slowly than  $1/r^2$  with distance from the first CR-39 detector. The observed deviation may be explained as a case of a nonlocal neutron source distributed inside the anode-cathode gap.

To clarify the source of the observed neutrons and the spatial domain of its emission requires further experimental investigation. In order to carry out the needed neutron energy spectrum measurements, a search for the locus or loci of the neutron emission should be done. These observations require a precision time-of-flight technique using additional neutron detectors based on <sup>3</sup>He and ZnS counters, and partial shielding of discharge area, and the application of different moderators and converters for increasing the neutron flux sensitivity in the different energy ranges. It is also important to perform measurements of possible neutron emission anisotropy. On the other hand, any influence of average and local electric fields and atmospheric parameters must be shown.

Currently, there is no reasonable model or mechanism to explain the generation of neutron bursts during atmospheric discharge in air. A special mystery is the origin of the neutrons with energies above 10 MeV.

The authors express their gratitude to S. M. Zakharov, V. A. Bogachenkov, and E. I. Saunin for assistance in conducting the experiments, and to A. V. Gurevich, S. S. Gershtein, and G. A. Mesyats for helpful discussions. The work was supported in part by the RFBR Grant No. 13-08-01379.

\*oginov@lebedev.ru

- [1] D. M. Smith, L. I. Lopez, R. P. Lin, and C. P. Barrington-Leigh, *Science* **307**, 1085 (2005).
- [2] V. P. Pasko, M. A. Stanley, J. D. Mathews, U. S. Inan, and T. G. Wood, *Nature (London)* **416**, 152 (2002).
- [3] A. N. Shyam and T. C. Kaushik, *J. Geophys. Res.* **104**, 6867 (1999).



- [4] M. Kuzhevskiy, Moscow Univ. Phys. Bull. **5**, 14 (2004), in Russian.
- [5] I. M. Martin and M. A. Alves, *J. Geophys. Res.* **115**, A00E11 (2010).
- [6] G. N. Shah, H. Razdan, G. L. Bhat, and Q. M. Ali, *Nature (London)* **313**, 773 (1985).
- [7] A. Chilingarian, A. Daryan, K. Arakelyan, A. Hovhannisyan, B. Mailyan, L. Melkumyan, G. Hovsepyan, S. Chilingaryan, A. Reymers, and L. Vanyan, *Phys. Rev. D* **82**, 043009 (2010).
- [8] A. Chilingarian, N. Bostanjyan, and L. Vanyan, *Phys. Rev. D* **85**, 085017 (2012).
- [9] H. Tsuchiya, K. Hibino, K. Kawata *et al.*, *Phys. Rev. D* **85**, 092006 (2012).
- [10] A. V. Gurevich, V. P. Antonova, A. P. Chubenko *et al.*, *Phys. Rev. Lett.* **108**, 125001 (2012).
- [11] L. S. Bratolyubova-Tsulukidze, E. A. Grachev, O. R. Grigoryan, V. E. Kunitsyn, B. M. Kuzhevskij, D. S. Lysakov, O. Yu. Nechaev, and M. E. Usanova, *Adv. Space Res.* **34**, 1815 (2004).
- [12] B. E. Carlson, N. G. Lehtinen, and U. S. Inan, *J. Geophys. Res.* **115**, A00E19 (2010).
- [13] R. L. Fleisher, J. A. Plumer, and K. Crouch, *J. Geophys. Res.* **79**, 5013 (1974).
- [14] L. P. Babich and R. A. Roussel-Dupre, *J. Geophys. Res.* **112**, D13303 (2007).
- [15] K. B. Eack, W. H. Beasley, W. David Rust, T. C. Marshall, and M. Stolzenburg, *J. Geophys. Res.* **101**, 29637 (1996).
- [16] A. V. Gurevich, G. M. Milikh, and R. Roussel-Dupre, *Phys. Lett. A* **165**, 463 (1992).
- [17] M. A. Uman, *The Lightning Discharge*, Int. Geophysics Series Vol. 39 (Academic, New York, 1987).
- [18] A. V. Agafonov, A. V. Oginov, and K. V. Shpakov, *Phys. Part. Nucl. Lett.* **9**, 380 (2012).
- [19] V. S. Belyaev *et al.*, *Phys. At. Nucl.* **72**, 1077 (2009).
- [20] A. M. Marenniy, N. A. Nefedov, and A. S. Rusetskiy, *Kratkie Soobshenia po Fizike FIAN*, N **6**, 42 (1998), in Russian.